Structures of Self-Assembled Monolayers of Aromatic-Derivatized Thiols on Evaporated Gold and Silver Surfaces: Implication on Packing Mechanism

Shun-Chi Chang, Ito Chao, and Yu-Tai Tao*

Contribution from the Institute of Chemistry, Academia Sinica, Taipei, Taiwan, Republic of China

Received January 12, 1994®

Abstract: Structures of self-assembled monolayers of 4′-alkoxybiphenyl-4-methanethiol, 4′-$CH_3(CH_2)_mOC_6H_4C_6H_4$-4-$CH_2SH$ (I), (6-alkoxynaphth-2-yl)methanethiol, 6-$CH_3(CH_2)_mOC_{10}H_6$-2-CH_2SH (II), and 4′-alkoxybiphenyl-4-thiol, 4′-$CH_3(CH_2)_mOC_6H_4C_6H_4$-4-SH (III) ($m$ = 15, 16) on surfaces of evaporated Au and Ag were characterized and compared with the corresponding structures of n-alkanethiol, $CH_3(CH_2)_mSH$ (IV) (m = 15, 16). The results revealed that compounds I, II, and III form well-ordered monolayers on Au and Ag, with nearly identical structure of the hydrocarbon tail, presumably because of the same herringbone packing of the aromatic chromophores on nearly identical lattices of Au and Ag substrates. The herringbone packing of the aromatic chromophores, supported by molecular mechanics calculations, in turn determines the lattice and the spacing of the hydrocarbon chains. That compounds I and III appear to have the same structure indicates that the binding geometry of sulfur can be either sp^3 (surface–S–C bond angle of ~109°) or sp hybridized (surface–S–C bond angle of ~180°), depending on packing interactions in other parts of the molecules. The least sterically demanding n-alkanethiol (IV) allows a greater density of packing on Ag but not on Au, causing the binding geometry of sulfur to the surface to differ on the two metals. The tighter packing of IV on Ag makes monolayers of thiols with short chains more ordered conformationally than those of Au.

Introduction

Self-assembled monolayers (SAMs) have been the subject of wide research activities recently both for their fundamental importance in understanding interfacial properties and for their potential applications in molecular technologies.[1] An understanding of the detailed structure of SAMs provides a molecular level correlation of structure and surface properties such as wetting,[2] adhesion,[3] lubrication, and catalysis.[4] Understanding the parameters that control the structure formation is also the first step toward further fine tuning of the structural features for specific applications such as optoelectronics and molecular electronics.[5] There are many systems that produce highly organized monolayer assemblies, such as silanes on hydroxylated surfaces, carboxylic acids on metal oxides, and alkanethiols on Au, Ag, or Cu. Among them, the adsorption of n-alkanethiols on Au(111) and Ag(111) surfaces is an extensively investigated SAM system.[6-11] Various techniques including FTIR,[10,11] Raman spectroscopy,[12] diffractions[13] of electrons, X-ray, or helium atoms, STM,[14] and AFM[15] were used to elucidate the molecular details of the structures of these monolayers. A consensus is that although the basic spacings of the lattices of these two substrates are very much similar (2.89 Å for Ag versus 2.88 Å for Au), the monolayer structures are different. On Au(111), an epitaxial $(\sqrt{3} \times \sqrt{3})$-R30° overlayer was formed with the thiolate head groups at an S···S spacing of 4.99 Å. The polymethylene chains tilt about 27° from the surface normal. On the surface of Ag(111), a chain tilt of ~12°, ~15°, or 3–8° is suggested in various works,[10-12,16] all much smaller than that proposed for the Au(111) system. The latest suggestion from surface plasmon Raman spectroscopy study gave 0 ± 5°.[17] A packing of chains with smaller lattice spacing and thus lesser chain tilt was proposed. The different behaviors found on Au and Ag are rationalized in terms of a restructured surface or multiple domains on silver. Nevertheless, earlier results[18,19] on adsorption of CH_3S on Ag(111) also showed an epitaxial structure with $(\sqrt{7} \times \sqrt{7})$R10.9° overlayer and an S···S distance of 4.41 Å. Thus there seems to be an intrinsic

* To whom correspondence should be addressed.

® Abstract published in *Advance ACS Abstracts*, June 15, 1994.

(1) For a general review, see: Ulman, A. *An Introduction to Ultrathin Organic Films*, Academic Press: Boston, 1991.

(2) (a) Bain, C. D.; Whitesides, G. M. *Angew. Chem., Int. Ed. Engl.* **1989**, *28*, 506–512. (b) Whitesides, G. M.; Laibinis, P. E. *Langmuir* **1990**, *6*, 87–96. (c) Laibinis, P. E.; Nuzzo, R. G.; Whitesides, G. M. *J. Phys. Chem.* **1992**, *96*, 5097–5105.

(3) (a) Chaudhury, M. K.; Whitesides, G. M. *Science* **1992**, *255*, 1230–1232. (b) Wasserman, S. R.; Biebuyck, H.; Whitesides, G. M. *J. Mater. Res.* **1989**, *4*, 886–892.

(4) Adamson, A. W. *Physical Chemistry of Surfaces*; Wiley: New York, 1976. (b) Somorjai, G. A. *Chemistry of Two Dimensions: Surfaces*; Cornell University Press: Ithaca, NY, 1981.

(5) Ulman, A. *Adv. Mater.* **1990**, *2*, 573–582.

(6) Porter, M. D.; Bright, T. B.; Allara, D. L.; Chidsey, C. E. D. *J. Am. Chem. Soc.* **1987**, *109*, 3559–3568.

(7) Finklea, H. O.; Avery, S.; Lynch, M.; Furtsch, T. *Langmuir* **1987**, *3*, 409–413.

(8) Nuzzo, R. G.; Zegarski, B. R.; Dubois, L. H. *J. Am. Chem. Soc.* **1987**, *109*, 733–740.

(9) Bain, C. D.; Troughton, E. B.; Tao, Y. T.; Evall, J.; Whitesides, G. M.; Nuzzo, R. G. *J. Am. Chem. Soc.* **1989**, *111*, 321–335.

(10) Laibinis, P.; Whitesides, G. M.; Parikh, A. N.; Tao, Y. T.; Allara, D. L.; Nuzzo, R. G. *J. Am. Chem. Soc.* **1991**, *113*, 7152–7167.

(11) Walczak, M. M.; Chung, C.; Stole, S. M.; Widrig, C. A.; Porter, M. D. *J. Am. Chem. Soc.* **1991**, *113*, 2370–2378.

(12) Bryant, M. A.; Pemberton, J. E. *J. Am. Chem. Soc.* **1991**, *113*, 3629–3637; 8284–8293.

(13) (a) Strong, L.; Whitesides, G. M. *Langmuir* **1988**, *4*, 546–558. (b) Dubois, L. H.; Zegarski, B. R.; Nuzzo, R. G. *J. Chem. Phys.* **1993**, *98*, 678–688. (c) Fenter, P.; Eisenberg, P.; Li, J.; Camillone, N., III; Bernasek, S.; Scoles, G.; Ramanarayanan, T. A.; Liang, K. S. *Langmuir* **1991**, *7*, 2013–2016. (d) Samant, M. G.; Brown, C. A.; Gordon, J. G., II. *Langmuir* **1991**, *7*, 437–439. (e) Chidsey, C. E. D.; Liu, G.; Rowntree, P.; Scoles, G. *J. Chem. Phys.* **1989**, *91*, 4421–4423.

(14) Widrig, C. A.; Alves, C. A.; Porter, M. D. *J. Am. Chem. Soc.* **1991**, *113*, 2805–2810.

(15) Alves, C. A.; Smith, E. L.; Porter, M. D. *J. Am. Chem. Soc.* **1992**, *114*, 1222–1227.

(16) Liang, K. S.; Fenter, P.; Eisenberger, P. *Phys. Rev. Lett.*, submitted for publication.

(17) Nemetz, A.; Fischer, T.; Knoll, W.; Ulman, A. *J. Phys. Chem.*, in press.

(18) (a) Rovita, G.; Pratesi, F. *Surf. Sci.* **1981**, *104*, 609–624. (b) Schwaha, K.; Spencer, N. D.; Lambert, R. M. *Surf. Sci.* **1979**, *81*, 273–284.

(19) Harris, A. L.; Rothberg, L.; Dubois, L. H.; Levinos, N. J.; Dhar, L. *Phys. Rev. Lett.* **1990**, *64*, 2086–2089.

0002-7863/94/1516-6792$04.50/0

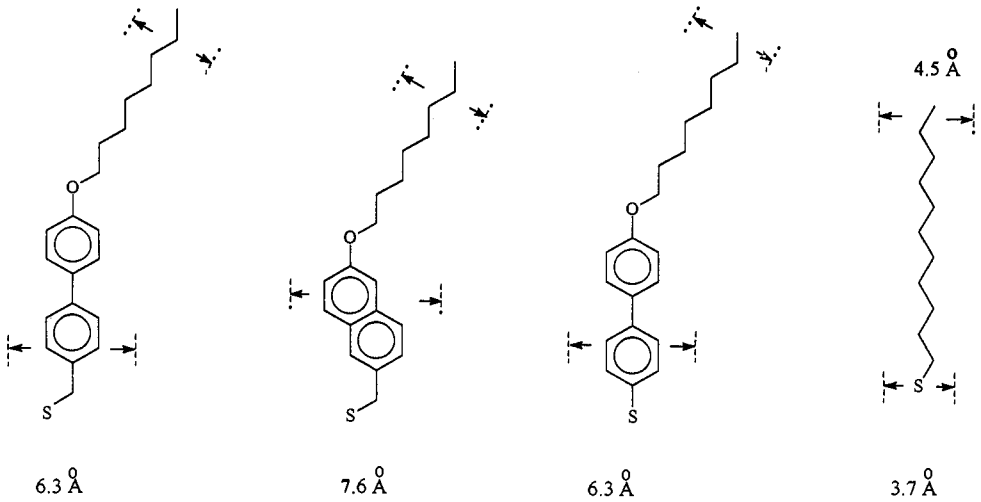

Figure 1. van der Waals diameters of I–IV.

difference in the binding patterns of thiol adsorbates on Au and Ag. Recently Ulman reported an *ab initio* calculation of the structure of thiolate binding to clusters of Au(111) and Ag(111).[20] The important conclusions from the calculation are that the thiolate on Au(111) can have two modes of chemisorption of similar energy, one with sp^3 hybridization at sulfur, giving a surface–S–C bond angle of ~104°, and another with sp hybridization at sulfur, giving a surface–S–C bond angle of ~180. The energy difference for binding at the "3-fold hollow" and "on-top" sites is smaller on Ag(111) than that on Au(111). It was proposed that *n*-alkanethiolate may have two binding modes, one with sp hybridization and the other with sp^3 hybridization, coexisting on Au(111) in a binding scheme involving only 3-fold hollow sites, so that the chain is highly tilted but the odd–even effect in IR spectra or wetting is diminished. On the other hand, *n*-alkanethiolate adopts a covering scheme in which on-top sites are also involved so as to have higher packing density and a smaller S···S spacing on silver.

Recently we reported a clear correlation of the odd–even effects in the IR intensities of the terminal methyl group and the odd–even effects in wetting properties of SAMs of carboxylic acid derivatives on Ag.[21,22] It was proposed that with the same, single binding mode, i.e., with the carboxylate head group bound symmetrically on silver, and the same binding lattice a different extent of chain tilt or chain twist may result due to the presence of an aromatic ring.[22] Here we report the effect of aromatic chromophores on structures of thiol monolayers and compare the monolayer structures of the same thiol on gold and silver. The adsorbates were 4′-alkoxybiphenyl-4-methanethiol, 4′-$CH_3(CH_2)_mOC_6H_4C_6H_4$-4-$CH_2SH$ (I), (6-alkoxynaphth-2-yl)-methanethiol, 6-$CH_3(CH_2)_mOC_{10}H_6$-2-CH_2SH (II), and 4′-alkoxybiphenyl-4-thiol, 4′-$CH_3(CH_2)_mOC_6H_4C_6H_4$-4-SH (II) ($m$ = 15, 16). The effect of a phenoxy group or a phenylsulfonyl group on the structures of SAMs was noted before,[23,24] and it was suggested that depending on the location of these chromophores, the assembly may or may not be ordered. The chain length above the aromatic ring appears to be important in determining the degree of orderedness of the assembly. Later it was suggested that the commensurability between *strata* of perturbing units and the chain segment is important in determining the ordering and packing of molecular assemblies.[25] In the present study, a biphenyl or naphthalene chromophore was introduced near the thiol head group to alter its steric requirements (Figure 1). A long hydrocarbon chain above the chromophore was used to probe the orderedness of the chain packing and the various head group packing. A pair of chain lengths (odd and even) was chosen because in a highly oriented system, the changing orientation of the terminal methyl group in an odd or even chain, manifested in IR intensities and wetting properties, provides valuable information concerning the "absolute" direction or sometimes the extent of chain tilt. A closer look at the odd–even effect found in the IR characteristics and wetting properties can reveal important information on the packing and orientation of these chains.

Intuitively, a larger head group would push away neighboring adsorbates so that a larger space is created between the alkyl chains above the head group, and the long tail groups might tilt more to make molecular contact. On the other hand, the binding sites on a surface can be very specific, with some sites more favored than the others. The flat aromatic chromophore may assume a specific arrangement in an ordered array. How the two factors match each other is at issue. The questions to be answered here are the following. How are these chromophores accommodated and arranged in the surface assembly, if they can indeed form an ordered assembly? How do these chromophores affect the packing and orientation of linear hydrocarbon chains connected to them? How do the structures vary on gold and silver? Compounds III, unlike compound I, has a sulfur atom directly attached to the biphenyl ring. The same binding geometry at sulfur for the two cases would yield different orientations of the aromatic chromophore. Or, conversely, the same orientation of the chromophores would require a different binding geometry at sulfur. By examining the spectroscopic and wetting data, information about the binding modes (or the surface–S–C bond angle) and the dominant force in these systems can be inferred. We include the SAMs of $CH_3(CH_2)_mSH$ (IV), even though it has been much investigated, for comparison. New insight, particularly about the short-chain thiols on Au and Ag, is suggested.

(20) Sellers, H.; Ulman, A.; Shnidman, Y.; Eilers, J. E. *J. Am. Chem. Soc.* **1993**, *115*, 9389–9401.
(21) Tao, Y. T. *J. Am. Chem. Soc.* **1993**, *115*, 4350–4358.
(22) Tao, Y. T.; Lee, M. T.; Chang, S. C. *J. Am. Chem. Soc.* **1993**, *115*, 9547–9555.
(23) Tillman, N.; Ulman, A.; Schildkraut, J. S.; Penner, T. L. *J. Am. Chem. Soc.* **1988**, *110*, 6136–6144.
(24) (a) Tillman, N.; Ulman, A.; Elman, J. *Langmuir* **1990**, *6*, 1512–1518. (b) Evans, S. D.; Urankar, E.; Ulman, A.; Ferris, N. *J. Am. Chem. Soc.* **1991**, *113*, 4121–4131.
(25) Shnidman, Y.; Ulman, A.; Eiler, J. E. *Langmuir* **1993**, *9*, 1071–1081.

Experimental Section

Materials. The solvents (absolute ethanol, tetrahydrofuran) were reagent grade. Pure water was obtained from a Barnstead Nanopure II system. Hexadecane was percolated twice through an alumina column. Compounds I–III were synthesized from 4-hydroxybiphenyl-4′-carboxylic acid, 6-hydroxy-2-naphthoic acid, and 4-bromo-4′-hydroxybiphenyl (all obtained from Tokyo Chemical Inc., Japan), respectively, according to literature or standard procedures (for details, see supplementary material). The purity of synthesized compounds was confirmed by ^{1}H-NMR, IR, and elementary analyses. Gold and silver metals used to prepare substrates were obtained from Johnson Matthey Electronics or Handy & Harman and were of 99.99% purity or higher. Single crystal silicon wafers (2-in. diameter) polished on one side were obtained from Semiconductor Processing Company (U.S.A.)

Substrate Preparation. The substrates were prepared by thermally evaporating (at a rate of 15–20 Å/s at 3×10^{-7} Torr using an Ulvac cryo-pumped evaporator) around 2000 Å of gold or silver onto the surfaces of 2-in. silicon wafers. An adhesion layer of chromium (50–100 Å) was evaporated prior to the evaporation of gold or silver. Films prepared under similar conditions were shown previously to be mainly of (111) texture.[10,26] After the substrates returned to room temperature, the vacuum chamber was back-filled with high-purity nitrogen. The substrates were either transferred directly to the adsorbing solution or placed into the solution right after the ellipsometric measurement was performed. The surfaces were exposed to the ambient atmosphere for 10 min at most. To minimize the effect of variable ambient exposures, batches of substrates were always freshly prepared and adsorptions of compounds in the same series were done concurrently.

Monolayer Preparation. Compounds I–III, due to lower solubility in ethanol, were dissolved in a mixture of ethanol and THF (1:1 v/v). Each compound was dissolved in THF first, and ethanol was added to make up the final solution at a concentration of 0.25 mM. Substrate wafers were placed in the solution for at least 10 h before being taken out for characterization. The wafers retrieved from the solution were washed with copious amounts of THF and ethanol successively and spun dry for various measurements.

Infrared Measurement. Reflection absorption IR spectra were taken with a Bomem MB-100 spectrometer equipped with an MCT detector. A custom-designed optics unit similar to that described in the literature[27] with 86° incidence angle using p-polarization was employed. A clean gold-coated wafer[28] was used as the reference for all spectra. A monolayer of perdeuterated docosanethiol on gold was used to check the cleanliness of the reference. One thousand scans were collected at 2-cm^{-1} resolution for signal averaging.

Contact Angle Measurement. Contact angles were measured with a Rame-Hart NRL Model 100 goniometer. The definition and method used to measure the static advancing contact angle θ_a are described in literature.[9] At least 3 drops of wetting liquid were measured for each sample, and the reported contact angle readings are the mean values from more than three batches of samples. The error of the contact angle of hexadecane was normally ~1° except in the range below 20°, where error may increase to 3°. Error in the contact angle value of water was ~2°.

Ellipsometry Measurement. A Rudolph AutoEL ellipsometer was used for the thickness measurement. The He–Ne laser (632.8 nm) light incidents at 70° on the sample and reflected into the analyzer. Data were taken over 3–5 spots on a given sample and averaged over3–5 batches of sample. A real index of refraction of 1.47 was assumed for all films in the calculation of the thickness.

Results

The ellipsometric thickness of various monolayers formed on Au and Ag are collected in Table 1. The thickness is approximately in the range expected for a monolayer with molecules aligned normal to the surface. For both metals, the thickness shows the order of I > II ~ III > V for the corresponding alkyl chain derivatives, which is in the same order as the "heights" of the aromatic chromophores. It was noted that for the same compound the apparent thickness on Au was invariably less than that on Ag, even in cases where other evidence indicates the same structure and orientation on the two surfaces. Direct comparison of thickness on different metals is probably unjustified because different systematic errors may be involved. For example, surface reactivity and thus extent of contamination may vary. It was also shown that an oxide layer is present on Ag before adsorption of thiol but largely disappears after monolayer coverage.[10] At the present level of accuracy and precision, the thickness measurement serves only as a qualitative indication of monolayer coverage. We also have reservations about the validity of estimating the degree of chain tilt based mainly on thickness data.

Table 1. Ellipsometric Thickness (Å) of Monolayers of I–IV on Au and Ag

	Au		Ag	
compd	$m = 15$	$m = 16$	$m = 15$	$m = 16$
I	32 ± 1	34 ± 1	35 ± 2	35 ± 1
II	29 ± 1	31 ± 1	31 ± 2	33 ± 2
III	30 ± 1	31 ± 1	32 ± 1	34 ± 1
IV	16 ± 1	18 ± 1	21 ± 1	22 ± 1

Table 2. Static Advancing Contact Angle (deg) on Monolayer of I–IV on Au and Ag

	Au				Ag			
	$m = 15$		$m = 16$		$m = 15$		$m = 16$	
compd	HD	H_2O	HD	H_2O	HD	H_2O	HD	H_2O
I	54	113	45	113	53	109	44	108
II	54	113	44	112	52	108	42	107
III	53	113	45	112	51	109	43	107
IV	52	112	50	111	51	109	52	109

Table 2 shows the static advancing contact angle θ_a for hexadecane and water on monolayers of I–IV on Au and Ag. The contact angle θ_a(HD) exhibits a strong dependence on the lengths of the hydrocarbon chains on monolayers of I–III, with θ_a (HD) on even-chain derivatives (m = 15) being 8–10° greater than that on odd-chain derivatives (m = 16). For monolayers of IV on Au, a difference of ~2° in θ_a(HD) on odd-chain and even-chain derivatives is probably meaningful (with an experimental error ±1°), Whereas on Ag, the contact angle is virtually the same. $\theta_a(H_2O)$ shows no such sensitivity to chain length on any monolayer.

Figures 2–5 show reflection–absorption infrared spectra of monolayers of compounds I–IV formed on Au and Ag. Transmission spectra of the corresponding compounds appear in Figure 6. For compounds I–III, the monolayer spectra on Au and Ag appear nearly identical (Figures 2–4). For example, in Figure 2a, a similarly significant odd–even effect was observed for the intensities of $\nu_s(CH_3)$ at 2878 cm^{-1} and $\nu_a(CH_3, ip)$ at 2963 cm^{-1} on both Au and Ag: the $\nu_s(CH_3)$ is larger for even-chain derivatives than for odd-chain derivatives, whereas the reverse is true for $\nu_a(CH_3, ip)$. The peak positions for the two methylene stretching modes $\nu_a(CH_2)$ and $\nu_s(CH_2)$ at 2919 and 2850 cm^{-1}, respectively, are indicative of an ordered assembly. Both the absolute and relative intensities of the two CH_2 modes are similar on the two metals. However, it is noted that the relative intensity of $\nu_s(CH_2)/\nu_a(CH_2)$ is clearly higher compared to that for *n*-alkanethiol on Au (Figure 5). Different optical constants for these two modes in different compounds are ruled out as judged from the spectra of isotropic samples (Figure 6). This effect should originate from orientation difference and is most likely due to different chain twist β along the molecular axis (see below). Compounds II and III gave the same patterns of variation as I on both Au and Ag. As the trend the extent of the odd–even effect relates to the absolute direction and to the extent of chain tilt or chain twist (see below), this observation suggests a similar

(26) Nuzzo, R. G.; Fusco, F. A.; Allara, D. L. *J. Am. Chem. Soc.* **1987**, *109*, 2358–2367.
(27) Allara, D. L.; Nuzzo, R. G. *Langmuir* **1985**, *1*, 45–52; 52–65.
(28) Ingrey, S.; Lau, W. M.; McIntyre, N. S. *J. Vac. Sci. Technol., A* **1986**, *4*, 984–988. Solomon, J. S.; Smith, S. R. *Proc. Mater. Res. Soc. Symp.* **1986**, *54*, 449–454.

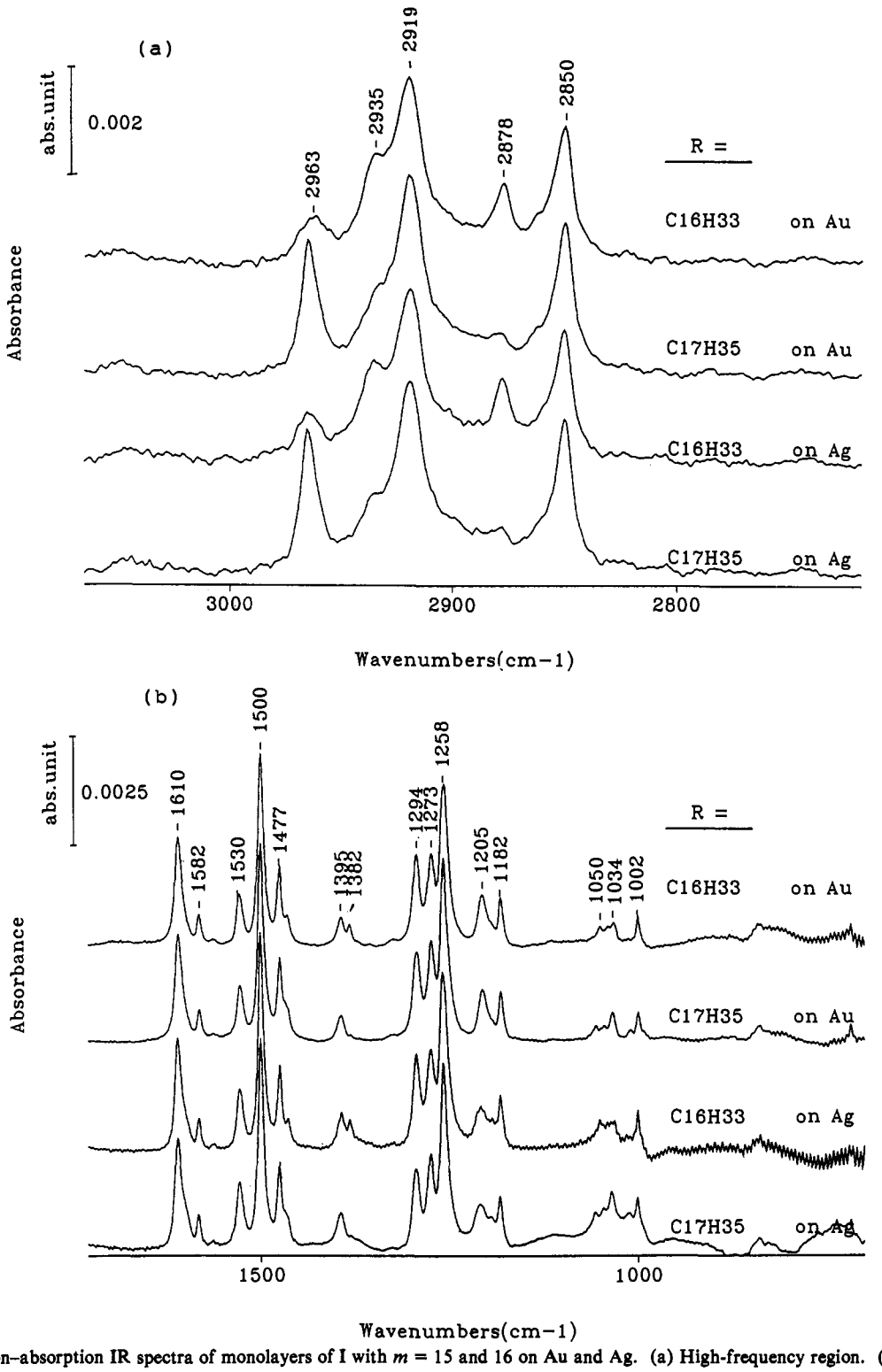

Figure 2. Reflection–absorption IR spectra of monolayers of I with m = 15 and 16 on Au and Ag. (a) High-frequency region. (b) Low-frequency region.

direction and extent of chain tilt for **I**, **II**, and **III**, even though different chromphores and chain lengths are involved. That is, I and II differ in the chromophore, whereas I and III differ in overall chain length, by one methylene unit next to the thiolate head group. The spectra in the low-frequency region also appear identical on Au and Ag for the same derivatives. For compound I (Figure 2b), the CH_3 deformation mode $\delta(CH_3)$ at 1382 cm^{-1} also shows an odd–even effect, clearly seen for the even-chain but not for the odd-chain spectrum. The trend of variation resembles that of $\nu_s(CH_3)$, again due to the same orientational origin because the transition dipoles of the two modes have the same direction. The most noteworthy is that the out-of-plane bending of the aromatic ring C–H at 826 and 809 cm^{-1} was absent, indicating little inclination of the plane of the ring toward the surface. Compounds II and III produced similar spectra on Au and Ag (Figures 3b and 4b). Again, the strong C–H out-of-plane bending mode observed in the isotropic sample was absent in the monolayer spectra of II and III. For III, there exist some fine differences; the single and broader peak at the 1474-cm^{-1} region on Au splits into two on Ag surface (Figure 4b).

Consistent with previous reports, IR spectra of IV on Au and Ag (Figure 5) are quite different. Absorptions associated with both asymmetric and symmetric CH_2 stretching modes are more intense for monolayers on Au than on Ag. On gold, a similar

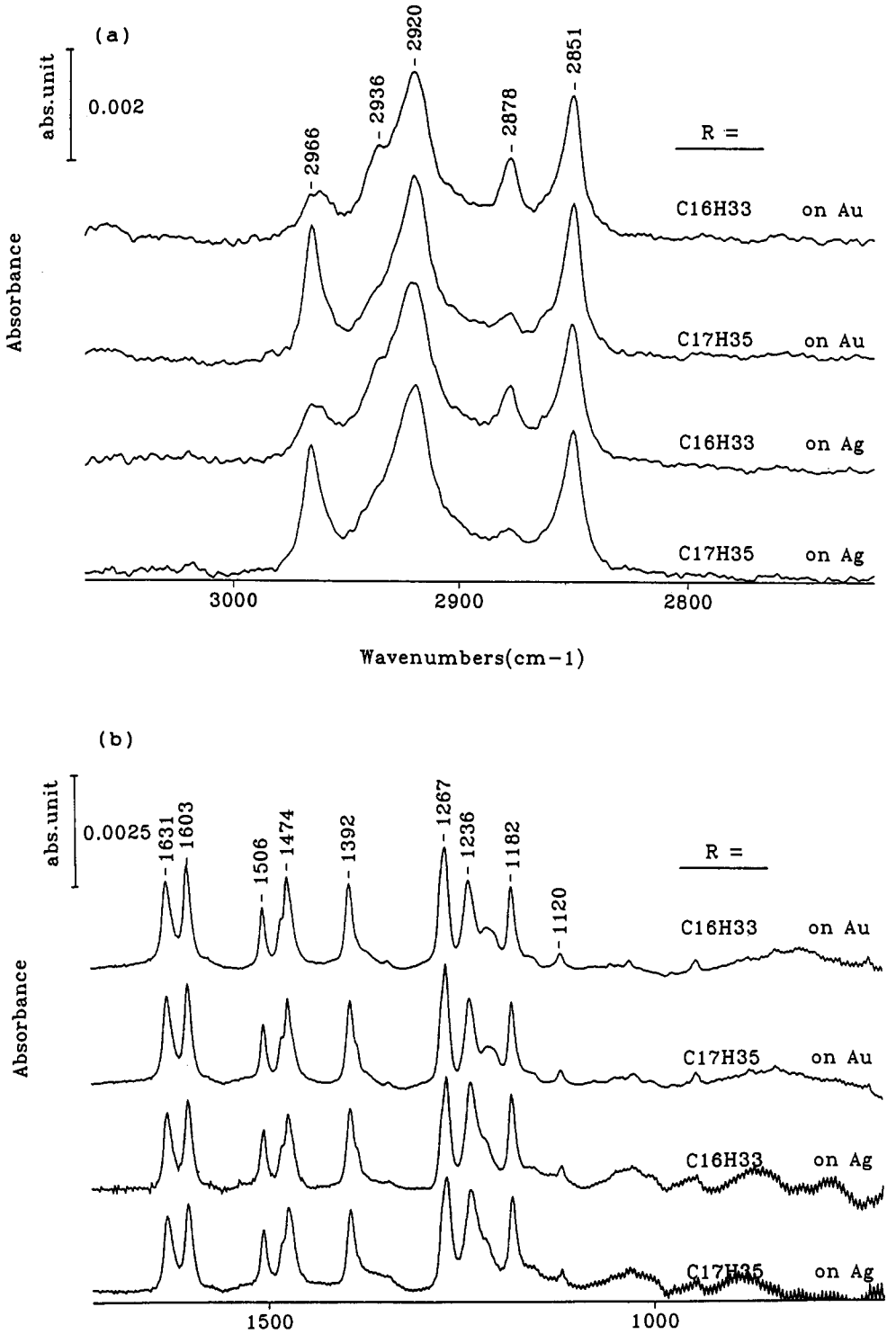

Figure 3. Reflection–absorption IR spectra of monolayers of **II** with $m = 15$ and 16 on Au and Ag. (a) High-frequency region. (b) Low-frequency region.

"odd–even" effect in the intensities of $\nu_s(CH_3)$ and $\nu_a(CH_3, ip)$ as observed in the spectra of **I–III** was found, but to a much lesser extent in the amplitude. On silver, variation of intensities of these two modes with chain length is very small. But as shown in our previous work,[22] a small but definite odd–even trend opposite to that observed for Au was found over a wider range of chain length. That is, the intensity of $\nu_s(CH_3)$ was greater for odd-chain thiols than for even-chain thiols, whereas the reverse was true for $\nu_a(CH_3, ip)$. In the low-frequency region, the peak associated with CH_2 deformation at 1465 cm^{-1} is also very weak in the case of Ag as compared to Au. The origin of this effect is expected to be the same as for the relatively low intensity associated with the symmetric CH_2 stretching vibration at 2849 cm^{-1}, because the two modes have the same direction of transition dipole. Progressional bands[29,30] (between 1150 and 1350 cm^{-1}) were discerned on both systems, indicating a *trans*-zigzag conformation for these long molecular chains.

The odd–even effect in wetting and IR spectra shows again a correlation: *the greater the odd–even alternation of intensity associated with methyl vibration modes, the greater the odd–even alternation of hexadecane contact angle.* That the odd–even effect in wetting of *n*-alkanethiol monolayer on Au or Ag

(29) Snyder, R. G.; Schachtschneider, J. H. *Spectrochim. Acta* **1963**, *19*, 85–117.

(30) Sheppard, N. *Advances in Spectroscopy*; Interscience: New York, 1959; Vol. I, p 288.

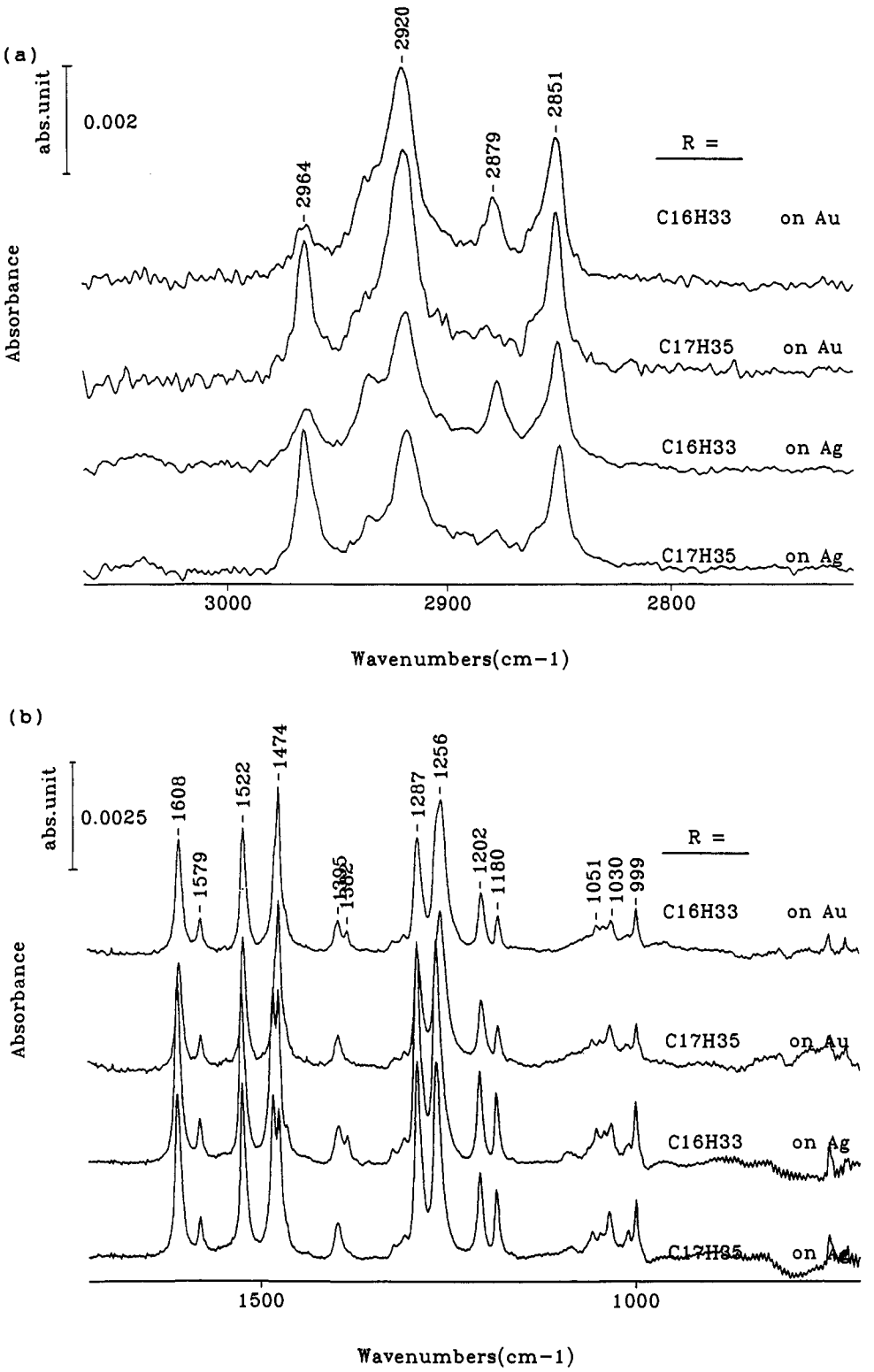

Figure 4. Reflection–absorption IR spectra of monolayers of III with $m = 15$ and 16 on Au and Ag. (a) High-frequency region. (b) Low-frequency region.

is ambiguous may correspond to a diminished odd–even effect in IR intensity.

Discussion

The molecules studied all have a long alkyl group connected through oxygen to an aromatic group, which is in turn connected to the surface through CH_2S or S. The alkoxy group is considered the tail group, whereas the aromatic group and below are taken to be the "effective" head group. The tail group and the "effective" head group constitute two distinct geometrical parts. The analysis of the geometries of these two parts with respect to the surface and their possible relations to IR spectral intensities and to wetting properties are considered separately.

Hydrocarbon Chain Geometry. As shown in Figure 7, the geometry of an *all-trans* polymethylene chain, whether attached to a surface through thiolate or through the ether linkage of the aromatic thiolate, can be described by a cant angle, α, defined as the cant of the molecular axis from the surface normal in the plane containing the *trans*-zigzag carbon skeleton, and an angle of chain twist, β, defined as the rotation of the plane containing

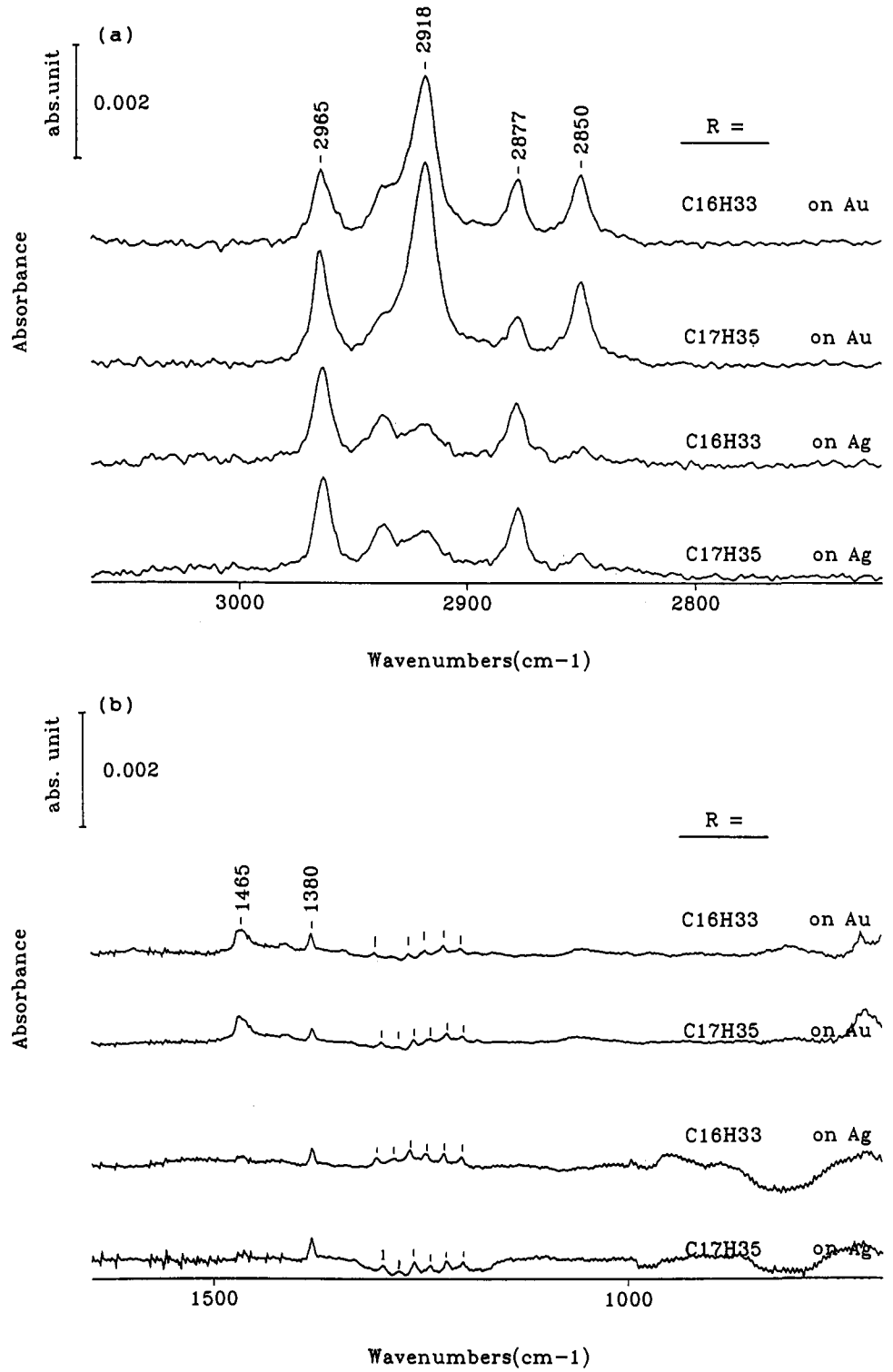

Figure 5. Reflection–absorption IR spectra of monolayers of IV with $m = 15$ and 16 on Au and Ag. (a) High-frequency region. (b) Low-frequency region.

the zigzag chain along the chain axis. For normal orientation ($\alpha = 0$), the terminal methyl group of either an odd chain or an even chain gives the same projection along the surface normal, and so do all the vibrational modes associated with it. The methyl-terminated surface is identical for an odd-chain or an even-chain system as viewed from the top or as sensed by a wetting liquid. The methylenes are all parallel to the surface plane. According to the selection rules of reflection IR spectroscopy[27] and the sensitivity of the wetting property to the structure of the top surface,[2] no odd–even effect in intensities of methyl vibration modes or contact angle is expected. However, as the chain tilts in the plane defined by the *trans* carbon skeleton ($\alpha \neq 0$), the top surface correspondingly varies between monolayer systems with odd-chain and even-chain derivatives. In the positive direction (defined to have the surface–S bond or the O–$C_{aromatic}$ bond aligned in a direction closer to the surface normal, z direction), the even carbon chain will have an increasing projection of the methyl group along the surface normal, and likewise the transition dipole of $\nu_s(CH_3)$. The $\nu_a(CH_3)$, being orthogonal to $\nu_s(CH_3)$, will have decreasing projection along the surface normal with increasing chain tilt. In contrast, the odd chain will have a decreasing z component of $\nu_s(CH_3)$ and an increasing z component of $\nu_a(CH_3)$ with increasing chain tilt. Such an opposite trend becomes increasingly significant with greater chain tilt. In

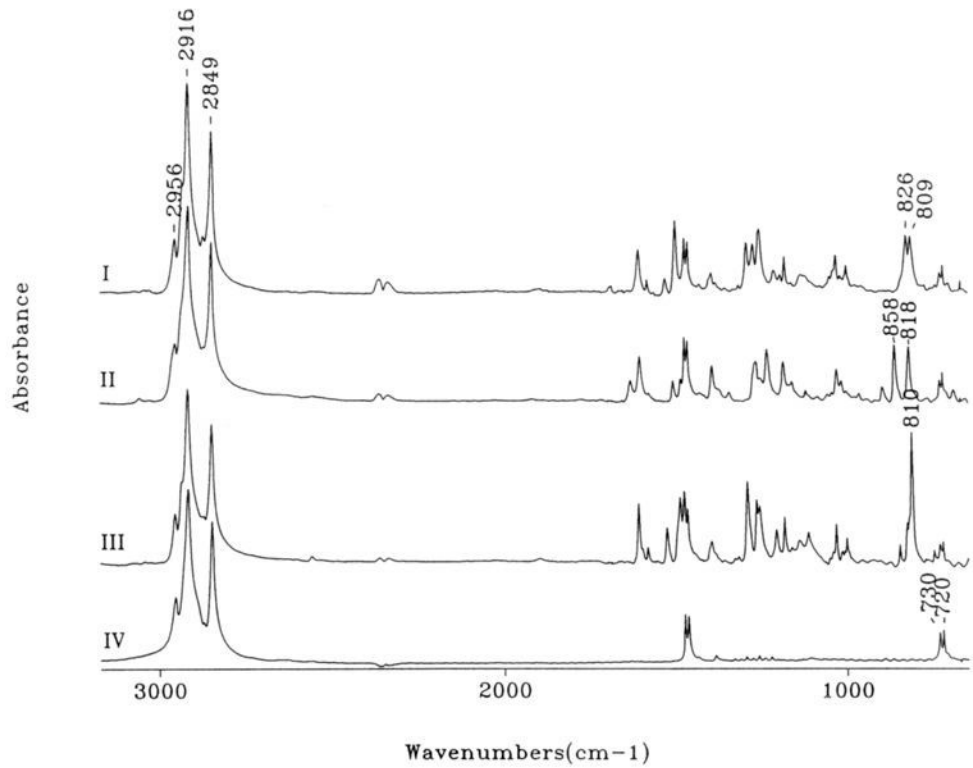

Figure 6. Transmission spectra of isotropic samples of (a) **I**, (b) **II**, (c) **III**, and (d) **IV** with $m = 15$.

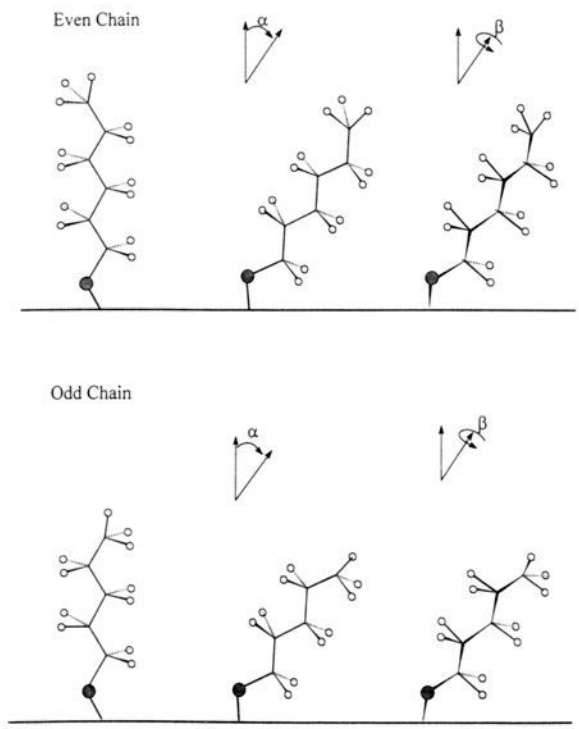

Figure 7. Schematic diagram of chain geometry of the polymethylene tail group relative to the surface.

both cases, the transition dipole of $\nu_s(CH_2)$ increases with increasing chain tilt. Viewed from the top, the even chain has less exposure of the methylene unit next to the terminal methyl group, whereas the odd chain has more exposure of the methylene unit. The wetting propety, particularly for a hydrocarbon liquid, was shown to be sensitive to such fine differences in structure.[21,22] When this analysis is applied to a negative tilt (defined to have the S–C_{alkyl} bond or the O–C_{alkyl} bond closer to the surface normal), all trends are reversed. Thus for even chains, the z component of the transition dipole of $\nu_s(CH_3)$ decreases with increasing chain tilt. Rotation about the molecular axis (increasing β), however, diminishes the divergence of both the z projections of the methyl group and the z components of transition dipoles of vibrational modes between odd and even chains. Increasing β also increases the z component of the transition dipole of $\nu_a(CH_2)$ at the expense of that of $\nu_s(CH_2)$. For example, a 90° chain twist totally smears out the odd–even effect in z components of $\nu_a(CH_3)$ and $\nu_s(CH_3)$ caused by any tilting angle and puts the z vector of $\nu_s(CH_2)$ to zero and that of $\nu_a(CH_2)$ to its maximum. As defined in previous simulations,[10,31] β is the rotation of the "plane" containing the *all-trans* chain. The rotation might occur progressively along the chain so that a slight deviation from *trans* conformation occurs at each methylene unit. The terminal methyl will then have more twist than the very beginning of the chain. It should be noted that the odd–even effect in IR spectra originates only from the methyl orientation changes and the odd–even effect in wetting originates only from the structure and orientation differences in the top 2–3-Å range.[2]

In a collection of linear and *trans*-zigzag alkyl chains, the molecular chain tilt is generally believed to relate to the spacing between chains, such that a greater tilt associates with a larger spacing.[31,32] The lattice spacing is determined by the chemisorption scheme on the surface. Ulman's calculation[31] suggests that only at a specific angle with a certain spacing can there be "interlocking" of the *trans*-methylene units. For other spacings, some combination of tilt and twist may be required to reach an energy minimum, depending on the balance of interchain and intrachain interactions, binding interaction, and binding geometry. Although Ulman's calculation was based on simple linear chains, in the presence of a structural perturbation such as an aromatic chromophore, the energy minimum may involve different tilt and twist *for the same spacing*. As the orientation of the terminal methyl group is related to both chain tilt and chain twist, it is

(31) Ulman, A.; Eilers, J. E.; Tillman, N. *Langmuir* **1989**, *5*, 1147–1152.
(32) Safran, S. A.; Robbins, M. O.; Garoff, S. *Phys. Rev. A* **1986**, *33*, 2188–2189.

possible to have different methyl orientation and thus a different odd–even effect in IR spectra and wetting for chains at *the same spacing*.

Head Group Geometry. The "effective" head groups constitute the second and apparently the dominant part of the packing process. For these aromatic derivatives, the question arises as to how the chromophores near the head groups arrange or orient themselves on the surface. Aromatic rings form either herringbone or face-stacked structures in a crystal, depending on their substituents and environment. X-ray data of biphenyl and naphthalene molecules, both of which have a herringbone structure in the crystalline state,[33,34] reveal that the distances between neighboring molecules are not significantly different from the $(\sqrt{3} \times \sqrt{3})R30°$ and $p(2 \times 2)$ lattice spacing of Au(111)[35] and that each molecule also has six neighbors in the direction perpendicular to the molecular plane.[36] Thus we performed molecular mechanics calculations[37] of the spatial arrangements of chromophores on a lattice corresponding to binding sites on the Au(111) surface. In our periodic model systems,[38] each unit cell contained four biphenyl or naphthyl molecules. In an attempt to simulate the binding phenomenon on metal surfaces, constrained minimizations were carried out with fixed H4 of biphenyl and H2 of naphthalene at distances equal to that between $(\sqrt{3} \times \sqrt{3})R30°$ Au(111) binding sites. The biphenyl H4–C4 bond vector and the naphthalene H2–C2 bond vector were aligned along the surface normal in initial geometries (Figure 8). Details of analyses will appear in a separate paper which focuses on computational results of current models and other aspects of SAM systems. In the present report, we briefly describe only the calculated chromophore packing chracteristics on the surface.

Our computational results indicate the herringbone arrangement to be favored over the face-stacked arrangement for both biphenyl and naphthalene systems with the 4.99-Å spacing of a $(\sqrt{3} \times \sqrt{3})R30°$ Au(111) lattice[39] (Figure 9). As naphthalene is larger than biphenyl according to van der Waals diameters (Figure 1), one might wonder if naphthalene packs better in a more expanded lattice, such as in a $p(2 \times 2)$ lattice. Minimizations of naphthalene fixed at a distance of 5.78 Å in a $p(2 \times 2)$ lattice still showed preference for the herringbone structure, but the energy gap between the herringbone and face-stacked arrangements decreased and the overall interaction energies were less favorable than those of the smaller lattice counterpart. Unlike

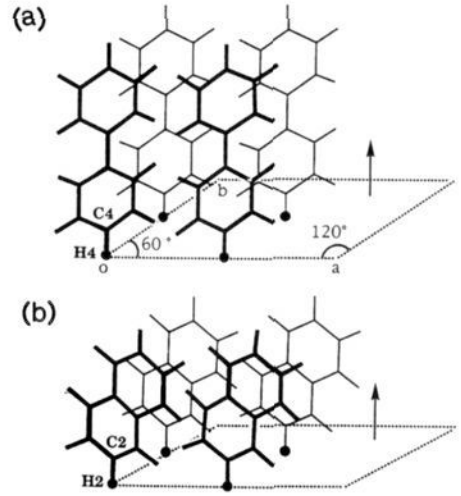

Figure 8. Examples of initial geometries of (a) biphenyl and (b) naphthalene periodic models for constrained optimizations. The darkened terminal hydrogens were fixed throughout optimizations. Cell parameters: $a = b = 9.98$ Å (twice the $(\sqrt{3} \times \sqrt{3})R30°$ lattice spacing), $c = 30$ Å, $\alpha = \beta = 90°$, $\gamma = 60°$.

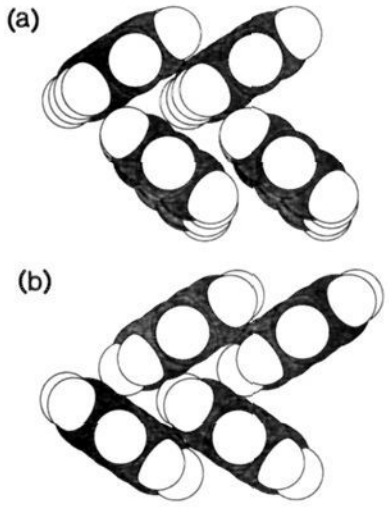

Figure 9. Calculated low-energy arrangements of (a) biphenyl and (b) naphthalene model systems, viewing down the surface normal. Only molecules in one unit cell are shown.

herringbone structures of biphenyl and naphthalene in the smaller lattice, the naphthalene ring plane tilted significantly away from the surface normal in order to increase intermolecular interactions in this expanded lattice. Surveys of the Cambridge Data Base showed that 4-hydroxybiphenyl,[40] 4′-dihydroxybiphenyl,[41] 2-naphthol,[42] and 2,6-dihydroxynaphthalene[43] all possessed herringbone structures. Therefore, this conclusion is expected to remain valid even if a substituted biphenyl or naphthalene was considered in the model systems. A perpendicular oriented biphenyl or naphthyl group dictates the direction of the O–$C_{aromatic}$ bond and C–$C_{aromatic}$ (in **I** and **II**) or S–$C_{aromatic}$ (in **III**) to be near the surface normal. A normal O–$C_{aromatic}$ bond direction in turn dictates the orientation of the terminal methyl group along a *trans*-zigzag chain. A tilted biphenyl or naphthyl group influences the direction of the methyl group of the same chain differently. Experimentally observed trends in the odd–even effect will give clues on the alignment of

(33) (a) Charbonneau, G. P.; Delugeard, Y. *Acta Crystallogr.* **1976**, *32*, 1420–1423. (b) Charbonneau, G.-P.; Delugeard, Y. *Acta Crystallogr., Sect. B* **1977**, *33*, 1586–1588.

(34) Brock, C. P.; Dunitz, J. D. *Acta Crystallogr., Sect. B* **1982**, *38*, 2218–2228.

(35) Using distances between terminal hydrogens defined in Figure 8 as references, the distances are in the range of 4.72–5.58 Å in the biphenyl crystal and 4.65–5.95 Å in the naphthalene crystal.

(36) The six neighbors form a distorted hexagon rather than a perfect hexagon with the $(\sqrt{3} \times \sqrt{3})R30°$ and $p(2 \times 2)$ lattices.

(37) Calculations were carried out with the UNIVERSAL force field in the program CERIUS v. 3.2. (It should be noted that the UNIVERSAL force field in version 3.2 does not completely correspond to the authentic force field yet. It is a hybrid of UNIVERSAL and DREIDING II force fields. Therefore, we added the following constraints to improve its performance: torsional constraints around sp^2 carbons to keep aromatic moieties planar and a bond length constraint for the C1–C1′ bond of biphenyl to keep this bond length in agreement with the experimental value.) In conjunction with charges generated by the charge equilibration method, this force field was found to afford reasonable cell parameters for benzene, biphenyl, and naphthalene crystals. References for UNIVERSAL, DREIDING II force fields and the charge equilibration method: Rappé, A. K.; Casewit, C. J.; Colwell, K. S.; Goddard, W. A., III; Skiff, W. M. *J. Am. Chem. Soc.* **1992**, *114*, 10024–10035. Casewit, C. J.; Colwell, K. S.; Rappé, A. K. *J. Am. Chem. Soc.* **1992**, *114*, 10035–10046. Mayo, S. L.; Olafson, B. D.; Goddard, W. A., III. *J. Phys. Chem.* **1990**, *94*, 8897–8909. Rappé, A. K.; Goddard, W. A., III. *J. Phys. Chem.* **1991**, *95*, 3358–3363.

(38) To simulate two-dimensional problems with three-dimensional periodic conditions, we assigned a large value (30 Å) to the unit cell parameter normal to the surface. Hence nonbonded interactions between successive layers were not included in the energy evaluation.

(39) In a recent report, the authors reached similar conclusion on a *p*-terphenyl mercaptan monolayer on Au(111): Sabatani, E.; Cohen-Boulakia, J.; Bruening, M.; Rubinstein, I. *Langmuir* **1993**, *9*, 2974–2981.

(40) Brock, C. P.; Morelan, G. L. *J. Phys. Chem.* **1986**, *90*, 5631–5640.

(41) Jackisch, M. A.; Fronczek, F. R.; Geiger, C. C.; Hale, P. S.; Daly, W. H.; Butler, L. G. *Acta Crystallogr., Sect. C* **1990**, *46*, 919–922.

(42) Watson, H. C.; Hargreaves, A. *Acta Crystallogr.* **1958**, *11*, 556–562.

(43) Bel'skii, V. K.; Kharchenko, E. V.; Sobolev, A. N.; Zavodnik, V. E.; Kolomiets, N. A.; Prober, G. S.; Oleksenko, L. P. *Zh. Strukt. Khim.* **1990**, *31*, 116–121.

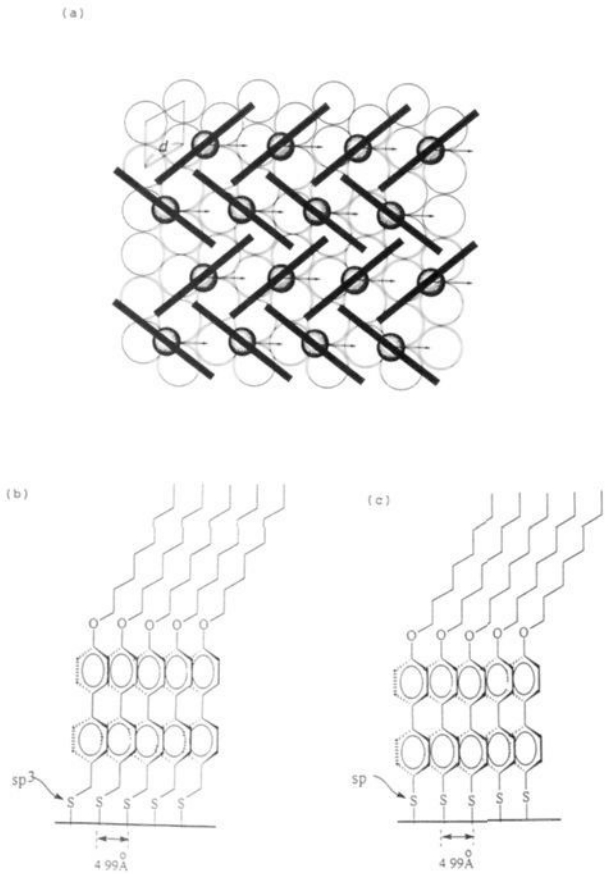

Figure 10. (a) Top view of proposed structures of monolayers of **I** and **III** on the $(\sqrt{3} \times \sqrt{3})R30°$ overlayer of Au(111) and Ag(111) surfaces. The arrows indicate the tilting direction of the alkyl chains. (b) Side view of monolayer of **I** along a line connecting the nearest neighbors. (c) Side view of monolayer of **III**.

these groups. The orientation of the aromatic ring will affect the relative intensities of various modes associated with the ring.

Among the series of four compounds, **IV** involves the smallest and simplest head group, the thiolate S^-. It is the hydrocarbon chain that sets the limit of packing, a spacing of 4.5 Å. All experimental results indicate the thiolates occupy the more favored 3-fold hollow sites in a $(\sqrt{3} \times \sqrt{3})R30°$ lattice on Au, presumably for greater gain in binding energy even though it is not optimum for packing of linear chains. Ulman's model calculation suggested that CH_3S can bind to Au(111) either by an sp^3 hybridization (surface–S–C angle 104°) or by an sp hybridization (surface–S–C angle 180°) with similar energy. Nonetheless, deviation from these two bond angles (at slightly higher energy) cannot be excluded if other packing interactions override. IR spectra could not yield information in this regard, although Raman study could.[12]

The observed results for various thiols can be rationalized as follows, bearing in mind that the $(\sqrt{3} \times \sqrt{3})R30°$ lattice is a favorable binding scheme for thiolate groups on Au(111). For **I** on the Au surface, we propose that the thiolate head groups also occupy a $(\sqrt{3} \times \sqrt{3})R30°$ lattice, because the favored herringbone packing of the biphenyl moiety closely matches the favored site lattice (Figure 10a). As shown in Figure 9, the biphenyl moiety in the herringbone structure has a vertical orientation, in good agreement with the IR observation that absorption for out-of-plane bending of aromatic C–H disappeared. Such an orientation can easily be accommodated by a sulfur adopting sp^3 hybridization (Figure 10b). Such an orientation also mandates a positive chain tilt for the tail group, which can be inferred from the trend in the odd–even effect in methyl mode intensities. The interchain interaction is only secondary in

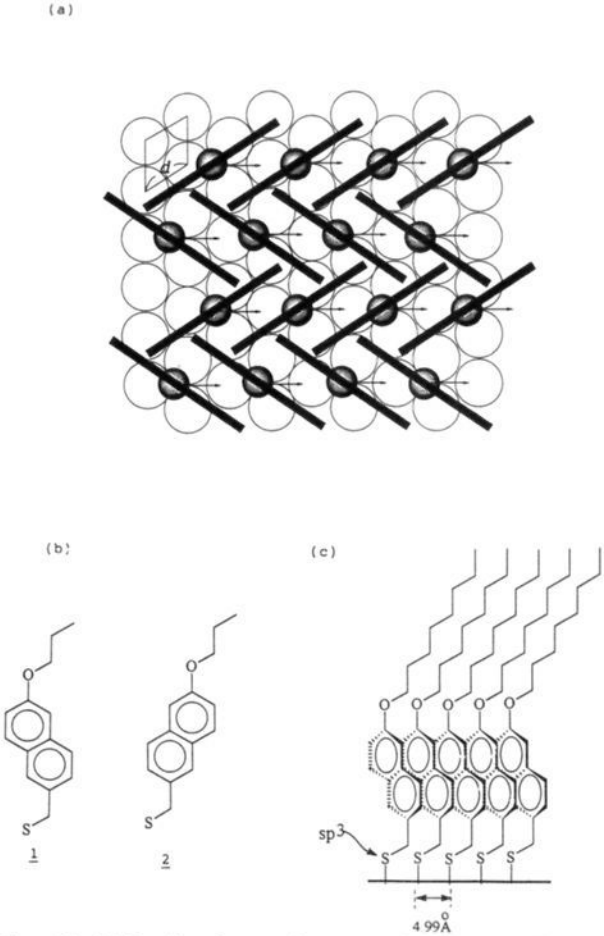

Figure 11. (a) Top view of proposed structure of monolayers of **II** on the $(\sqrt{3} \times \sqrt{3})R30°$ overlayer of Au(111) and Ag(111) surfaces. The arrows indicate the tilting direction of the alkyl chains. (b) Four conformations for the head group. (c) Side view of the monolayer along a line connecting the nearest neighbors.

determining the packing lattice in this case. In fact, even when the tail is a short chain such as a C4 or C5 group, the same odd–even patterns and intensities for the alkyl chain and the aromatic chromophore were observed, indicating the same chromophore packing and equally ordered hydrocarbon assembly (Figure 14 and further elaboration on short-chain systems later). The hydrocarbon chains above the aromatic ring tilt and rotate to maximize interchain interactions. Tail groups of odd-chain and even-chain systems have different orientations for the methyl group and different exposure of the methylene unit adjacent to the terminal methyl groups. Organic wetting liquids, such as hexadecane, bicyclohexyl, etc., reflect this condition by exhibiting an odd–even effect in the contact angle, higher on the surface with less methylene exposure and lower on the surface with more methylene exposure.[21,22] Silver has virtually the same basic lattice as gold. Compound **I** on Ag gave nearly identical IR spectral characteristics and wetting properties. Hence **I** on Ag also adopts a $(\sqrt{3} \times \sqrt{3})R30°$ overlayer and makes the same tilt and twist for the tail hydrocarbons. For **II** on Au and Ag, the $(\sqrt{3} \times \sqrt{3})R30°$ lattice (Figure 11a) is also adopted because **II** and **I** gave the same odd–even effect in both IR spectra and the wetting property and the same relative intensities of $\nu_s(CH_2)$ and $\nu_a(CH_2)$ modes. For the naphthyl head group region, various conformations are possible due to the eclipsing effect of the single

(44) This is the one with $O–C_{alkyl}$ bond eclipsing in a direction where more double-bond character on the aromatic ring occurs. Nevertheless, the energy difference relative to **2** is small (less than 1 kcal/mol). The packing interaction in the assembly, as suggested in the text, can drive the eclipsing bond off the ring plane, making the energy difference even smaller.

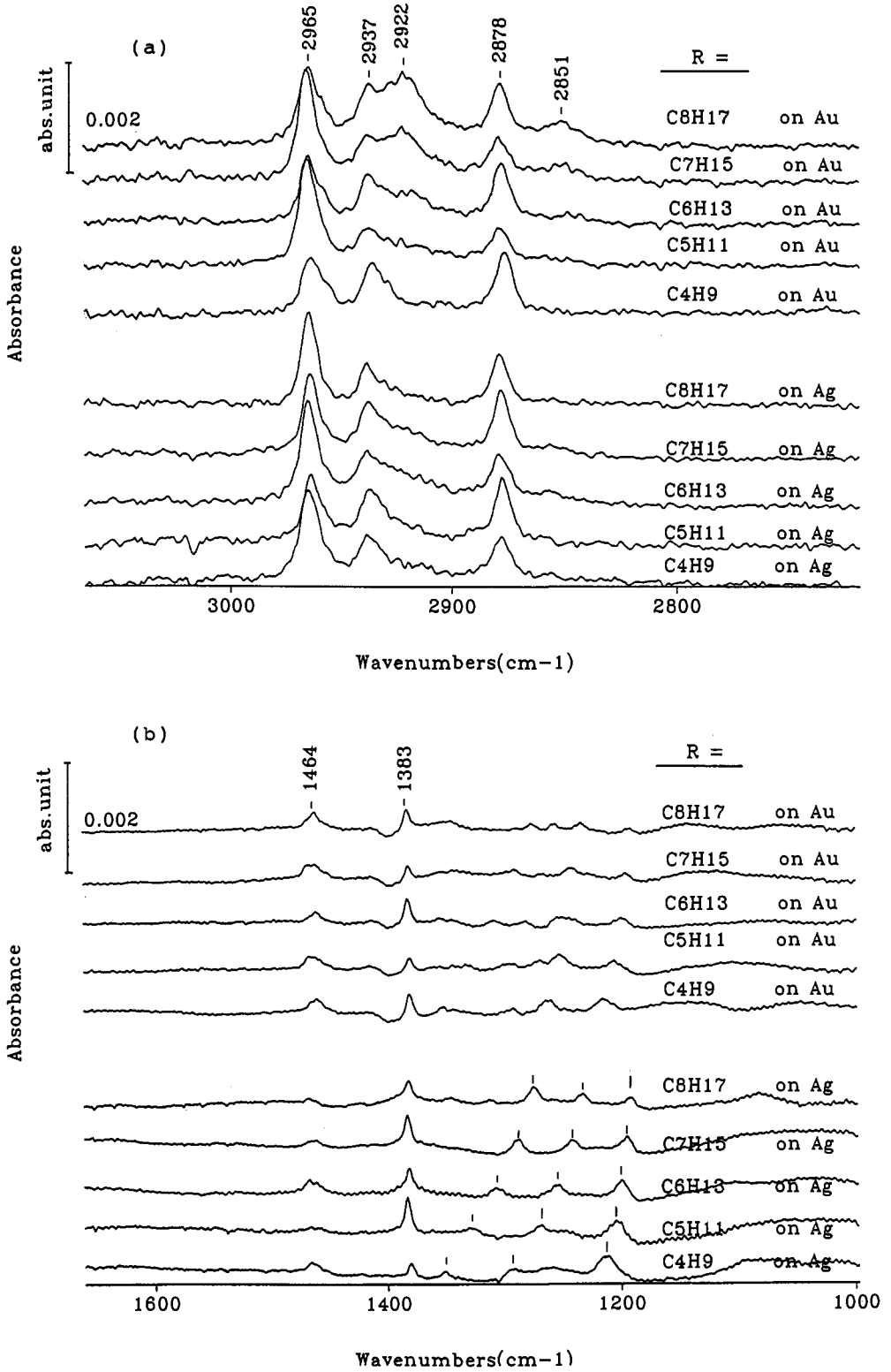

Figure 12. Reflection–absorption IR spectra of monolayer of **IV** (with $m = 3$–7) on Au and Ag. (a) High-frequency region. (b) Low-frequency region.

bond with aromatic rings, with 1 (shown in Figure 11b) slightly lower in energy relative to others according to molecular dynamics calculation.[44] Adoption of any one or a mixture of these will give indistinguishable IR, wetting, and ellipsometric results and will not change the interpretation of the structure of the tail group region.

Compound **III** exhibits IR spectra and wetting behavior similar to those of **I**, indicating that the two must have similar chain tilts and directions of chain tilt, hence similar orientation of the biphenyl group, i.e., perpendicular to the surface. This compels the conclusion that a different binding mode for sulfur on the same $(\sqrt{3} \times \sqrt{3})R30°$ lattice occurs, via either different hybridization of the sulfur atom or a greatly distorted bond angle (Figure 10c). Such a change of binding geometry can result from overriding packing interaction of the aromatic rings.

How can these systems have a much stronger odd–even effect than that for *n*-alkanethiols on Au if they all occupy the same $(\sqrt{3} \times \sqrt{3})R30°$ lattice structure and thus have the same lattice spacing of the hydrocarbon chains? The cause should be related to the phenyl ring. As shown in Figures 10 and 11, for the reason of symmetry, the chains are depicted as pointing toward the nearest neighbors. A rotational barrier is involved due to the eclipsing

effect of the O–C_{alkyl} bond on the ring plane,[45,46] a condition not existing in the case of *n*-alkanethiolate on the same surface. This constraint alters the energetics of interchain interaction and may lead to a different chain twist at the same chain tilt. Comparing the relative intensities of methylene stretching modes in the spectra of I, II, III, and IV supports a higher chain twist in the case of *n*-alkanethiolate on Au than in the other three cases because the intensity of $\nu_a(CH_2)$ increases at the expense of that of $\nu_s(CH_2)$ in the spectra of IV (see discussion above). Hence the same large chain tilt but a diminished odd–even effect is well accommodated by a highly twisted chain. To rationalize the diminished odd–even effect observed on SAM of IV, Ulman suggested the coexistence of two equally stable chemisorption modes, sp^3 and sp hybridization on the sulfur atom. The relative population was suggested to be dependent on the preparation protocols in various laboratories. However, the mode with sp hybridization will give the *opposite* direction in the odd–even effect at the same tilt. A "positive" trend is always observed, suggesting that the sp^3 mode is always more favored. For this scheme to be valid, there has to have a mixed surface environment in which one (that favors sp^3 hybridization) is invariably dominant.

In the absence of a phenyl ring, structures of linear alkanethiolate on Au and Ag start to diverge. Results show that *n*-alkanethiols still adopt the $(\sqrt{3} \times \sqrt{3})R30°$ lattice on Au(111), whereas on Ag a nearly normal orientation of the chains occurred, hence the interchain spacing and lattice spacing of the binding sulfur are necessarily decreased. The sulfurs bind more densely on Ag(111) than on Au(111) because, according to Ulman's calculation and suggestion, the energy difference between the 3-fold hollow sites and the on-top sites on Ag(111) surface is smaller than that on Au—3.3 versus 6 kcal;[20] thus some thiols can adopt the on-top sites, and the penalty in energy paid for by the gains in more interchain interactions and surface binding energy. If the driving force for denser packing comes mainly from interchain interaction, which may be comparable to binding energy in cases of longer chains,[8] it is expected to be chain length-dependent, such that the short-chain thiols on Ag might adopt the same lattice as short-chain thiols on Au and transform to a compressed lattice as the cohesive interchain interaction increases. If the driving force comes mainly from gains in binding energy, the packing density will be the same for chains of all lengths. Walczak *et al.*[11] reported an intriguing "diminution" of the odd–even effect in both IR spectra and contact angle of long-chain thiols relative to those of short-chain thiols on Ag. This dependence fits the expectation of an altered binding lattice (a more tilted chain, thus a greater odd–even effect, in a larger lattice transforming to a near-normal chain, thus a smaller odd–even effect, in a tighter lattice). This proposition is excluded on further examination. We examined carefully the short-chain thiols on Au and Ag; the spectra appear in Figure 12. For Au, no clear diminution of odd–even effects in IR intensities of the methyl modes was found in going from short-chain thiols to long-chain thiols. The absolute intensities for the methyl modes were also very much similar for all odd chains or even chains. However, some decrease of the odd–even effect was found for Ag for longer chains relative to that for short chains. The "opposite" direction of the trend in odd–even effect from the two surfaces was evident from both the CH_3 stretching modes and the deformation mode at 1383 cm^{-1}. In addition, progressional bands are obscure for these short-chain thiols on Au but clear on Ag, indicating a *trans*-zigzag conformation on the latter![47] The contact angle also shows

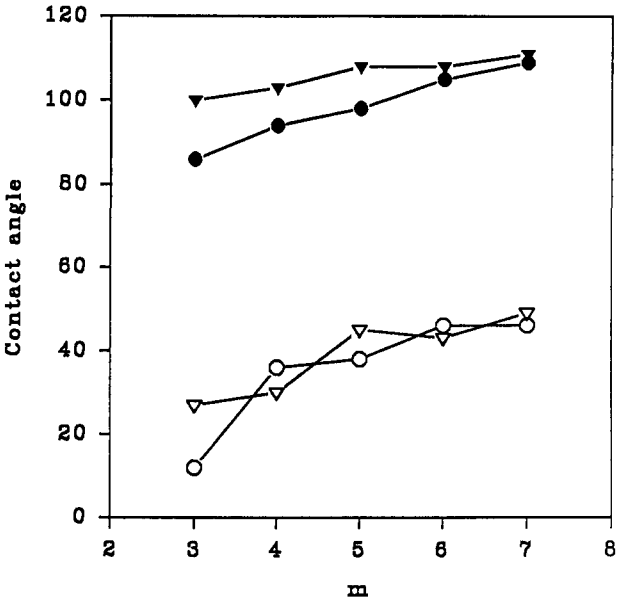

Figure 13. Contact angle on monolayers of IV (with m = 3–7) on Au and Ag. ▽, ▼ for values on Au surface; ○, ● for values on Ag surface. Filled symbols denote $\theta_a(H_2O)$; open symbols denote $\theta_a(HD)$.

an odd–even effect in opposite directions for Au and Ag (Figure 13), more significant for hexadecane than for water. The trend of alternation in contact angle appears to diminish with increasing chain length. This is compounded by the substrate effect due to the thinness of the films.[48] All data indicated that the structures on Au and Ag are different for both short- and long-chain thiols. The trend of variation on Au is consistent with a positive tilt of the chains, but on Ag, the small but definite "opposite" direction of the odd–even trend indicates an opposite or "negative" tilt. The "negative" tilt may result from sp hybridization on sulfur.[49] Furthermore, we propose that on silver the chain spacing is smaller and there is little room for the chains to move around; thus the assembly is more ordered conformationally and the progressional bands are readily detected. The reason for the odd–even effect diminishing for long chains relative to short chains, we believe, is the rotation of the chain. As discussed above, rotation can diminish variation in methyl orientation between odd chains and even chains incurred due to chain tilt. Yet the rotation can be progressive so that the end of a longer chain may rotate more than the end of a shorter chain. The odd–even effect relates only to the end of the chain. An odd–even effect diminishing with chain length supports a greater rotation of the end of a long chain than the end of a short chain, with respect to the base. That a shorter chain assembly exhibits a greater odd–even effect was also observed in monolayers of I. Figure 14 shows spectra of monolayers of I with a C4 and C5 chain. For a chain as short as C4, the whole assembly is well ordered. The contact angle $\theta_a(HD)$ on a C4-substituted I is greater than that on a C5-substituted one (51° versus 43°, respectively). The biphenyl-related peaks and intensities are nearly identical to those of long chain-derivatives. However, the CH_3 deformation band at 1383 cm^{-1} and the stretching modes in the high-frequency region clearly

(45) Allen, G.; Fewster, S. In *Internal Rotations in Molecules*; Orville-Thomas, W. J., Ed.; Wiley: New York, 1974.

(46) Spellmeyer, D. C.; Grootenhuis, P. D. J.; Miller, M. D.; Kuyper, L. F.; Kollman, P. A. *J. Phys. Chem.* **1990**, *94*, 4483–4491.

(47) Contrary to the common belief that a monolayer with shorter chains is less dense and disordered,[6,9] it should be as highly oriented and "equally dense" as one with longer chains. That HS or CH_3SH can give a more compressed $(\sqrt{7} \times \sqrt{7})R10.9°$ lattice is the best example to show that adsorption density has nothing to do with chain length in this case.

(48) Just how the substrate affects the contact angle is unclear. But it can be seen that any major jump in contact angle comes about when there is a greater increase in thickness associated with the additional unit of methylene. For example, for the Au surface, going from C5 thiol to C6 thiol, the thickness increases by an amount close to the length of a C–C bond, or 1.41 Å. In going from C6 to C7, the thickness increases by an amount close to a fraction (~cos 70°) of the C–C bond. For Ag, there is a greater increase of thickness in going from C4 to C5 than from C5 to C6. This effect indicates the high sensitivity of the contact angle to the thickness of the screening layer in this range of thickness.

(49) In this sense, the term "negative" tilt showed be abandoned. The chain can be described by the same tilting direction as on Au, except a different bond angle at the sulfur head makes the orientation of the terminal group different.

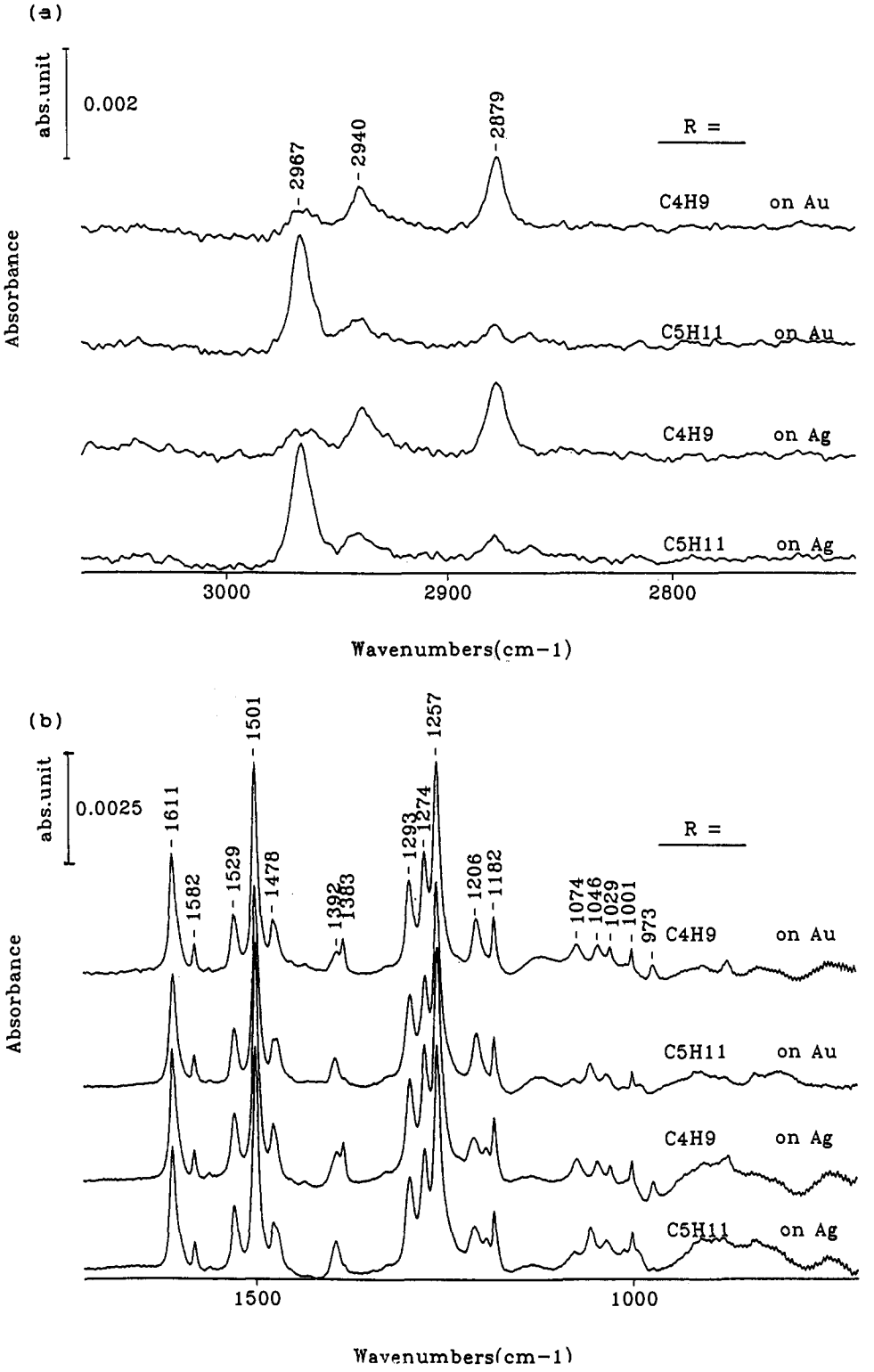

Figure 14. Reflection–absorption IR spectra of monolayers of I with $m = 3$ and 4 on Au and Ag. (a) High-frequency region. (b) Low-frequency region.

show a larger odd–even effect than that shown in Figure 2. The packing of the effective head group is expected to be the same; thus the phenomenon of diminishing odd–even effect is the result of greater rotation of the end of longer chains than that of shorter ones.

For *n*-alkanethiolate on gold, the interchain spacing is larger, and there is insufficient cohesive interaction for the short-chain thiols to hold tightly together so as to give signals in diffraction measurement,[13d] even though the same ordered lattice pattern of C2 and C18 thiols was found by STM.[14] A better description of short-chain thiols on Au would be a liquid crystalline state with two-dimensional order in terms of the surface lattice, in which the chains can precess (through *trans*-gauche interconversion) while maintaining an average tilt. A short chain *n*-alkanoic acid adsorbed on silver also gives conformational order,[22] although the tilt is similar to that of a short thiol on Au. The reason is proposed to be the rotational barrier (eclipsing effect of C_2–C_3 bond on the C–O bond of the carboxylate group[50])-that hinders the precessing of chains.

(50) Burkert, U.; Allinger, N. L. *Molecular Mechanics*; ACS Monograph Series 177; American Chemical Society: Washington, DC, 1982, Chapter 6.

Conclusion

The adsorption of various thiol derivatives on Au and Ag provides a test ground of interplay of various interactions involved in the process of self-assembling. With nearly the same lattice parameters of Au and Ag, the monolayer structures are also the same for the aromatic-containing thiols because the packing arrangement of the aromatic chromophores becomes dominant. Molecular mechanics calculations indicate that the 4,4′-substituted biphenyl or 2,6-substituted naphthyl in **I–III** can form a herringbone structure that is commensurate with the $(\sqrt{3} \times \sqrt{3})R30°$ lattice. The aromatic ring imposes a new constraint and affects the energetics of rotation of the molecular chain so that varied orientation of the terminal methyl group and thus varied odd–even effect can result for the *same* lattice spacing. In SAMs of **III**, the binding geometry yields to the packing interaction. The adsorption scheme and structure for *n*-alkanethiol becomes different on Au and Ag because the least sterically demanding linear chain allows a denser packing scheme in addition to the $(\sqrt{3} \times \sqrt{3})R30°$ lattice. This denser packing indeed takes place on silver because the energy gain in having a denser packing overcomes the energy cost in involving less favorable sites, whereas on Au, the energy gain cannot compensate the energy cost. Short chain length does not preclude ordered packing. Depending on the packing density and/or presence of a rotational barrier, *trans*-zigzag conformational order can occur, such as in the case of short-chain thiols on Ag and short-chain acids on Ag.

Acknowledgment. Financial support from National Science Council, Republic of China, is gratefully acknowledged.

Supplementary Material Available: Scheme for the syntheses of **I–III** followed by a description of the procedures and characterization data (5 pages). This material is contained in many libraries on microfiche, immediately follows this article in the microfilm version of the journal, and can be ordered from the ACS; see any current masthead page for ordering information.